In situ and experimental evidence for acidic weathering of rocks and soils on Mars

J. A. Hurowitz,[1] S. M. McLennan,[1] N. J. Tosca,[1] R. E. Arvidson,[2] J. R. Michalski,[3] D. W. Ming,[4] C. Schröder,[5] and S. W. Squyres[6]

Received 20 June 2005; revised 13 September 2005; accepted 21 September 2005; published 6 January 2006.

[1] Experimental data for alteration of synthetic Martian basalts at pH = 0–1 indicate that chemical fractionations at low pH are vastly different from those observed during terrestrial weathering. Rock surface analyses from Gusev crater are well described by the relationships apparent from low-pH experimental alteration data. A model for rock surface alteration is developed, which indicates that a leached alteration zone is present on rock surfaces at Gusev. This zone is not chemically fractionated to a large degree from the underlying rock interior, indicating that the rock surface alteration process has occurred at low water to rock ratio. The geochemistry of natural rock surfaces analyzed by APXS is consistent with a mixture between adhering soil/dust and the leached alteration zone. The chemistry of rock surfaces analyzed after brushing with the RAT is largely representative of the leached alteration zone. The chemistry of rock surfaces analyzed after grinding with the RAT is largely representative of the interior of the rock, relatively unaffected by the alteration process occurring at the rock surface. Elemental measurements from the Spirit, Opportunity, Pathfinder, and Viking 1 landing sites indicate that soil chemistry from widely separated locations is consistent with the low-pH, low water to rock ratio alteration relationships developed for Gusev rocks. Soils are affected principally by mobility of Fe and Mg, consistent with alteration of olivine-bearing basalt and subsequent precipitation of Fe- and Mg-bearing secondary minerals as the primary control on soil geochemistry.

Citation: Hurowitz, J. A., S. M. McLennan, N. J. Tosca, R. E. Arvidson, J. R. Michalski, D. W. Ming, C. Schröder, and S. W. Squyres (2006), In situ and experimental evidence for acidic weathering of rocks and soils on Mars, *J. Geophys. Res.*, *111*, E02S19, doi:10.1029/2005JE002515.

1. Introduction

[2] The petrography, mineralogy and geochemistry of sedimentary rocks have long been utilized for the reconstruction of environmental conditions in the Earth's past [e.g., *McLennan et al.*, 1993; *Nesbitt and Young*, 1982; *Patchett et al.*, 1999]. Accordingly, the chemical and mineralogical changes that accompany weathering of the Earth's crust have been studied in great detail in order to better understand the processes controlling the composition of sedimentary rocks [*Nesbitt and Markovics*, 1997; *Nesbitt and Young*, 1984; *Nesbitt et al.*, 1996]. In particular, the weathering of granodiorite has received much attention, since the Earth's upper continental crust is known to be, on average, of granodioritic composition [*McLennan*, 2001; *Taylor and McLennan*, 1985]. Although it has received less consideration, the weathering of basaltic rocks on Earth has been studied as well, and there is a reasonable understanding of the bulk chemical and mineralogical changes that accompany the alteration of such rocks under terrestrial conditions [*Eggleton et al.*, 1987; *Gislason et al.*, 1996; *Gislason and Eugster*, 1987; *Nesbitt and Wilson*, 1992]. With the advent of in situ geochemical and mineralogical study of Martian rocks and soils (Viking, Pathfinder, MER), it has become possible to investigate the alteration of basaltic rocks and soils on that planet. Interestingly, altered Martian rocks and soils do not appear to have evolved in a manner consistent with alteration of basalts as we know it on Earth [*McSween et al.*, 2003; *McSween and Keil*, 2000].

[3] Here we present new findings regarding weathering processes on Mars utilizing the results of alteration experiments performed at low pH on synthetic basalts of Martian composition [*Hurowitz et al.*, 2005; *Tosca et al.*, 2004]. These experimental results indicate that weathering in the low-pH environment thought to be important for Martian surface waters [*Banin et al.*, 1997; *Burns*, 1993; *Clark and Van Hart*, 1981; *Haskin et al.*, 2005; *Squyres et al.*, 2004;

[1]Department of Geosciences, State University of New York at Stony Brook, Stony Brook, New York, USA.
[2]Department of Earth and Planetary Sciences, Washington University, St. Louis, Missouri, USA.
[3]Department of Geological Sciences, Arizona State University, Tempe, Arizona, USA.
[4]NASA Johnson Space Center, Houston, Texas, USA.
[5]Institut für Anorganische und Analytische Chemie, Johannes Gutenberg-Universität, Mainz, Germany.
[6]Department of Astronomy, Cornell University, Ithaca, New York, USA.

0148-0227/06/2005JE002515$09.00

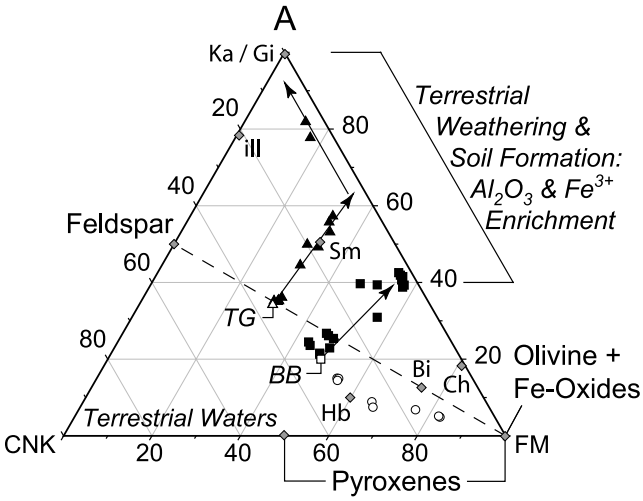

Figure 1. Ternary FeO_T + MgO (FM), Al_2O_3 (A), CaO + Na_2O + K_2O (CNK) diagram; data plotted in mole percent. White triangle (labeled TG) is unaltered Toorongo granodiorite, black triangles are the Toorongo granodiorite weathering profile; white square (labeled BB) is unaltered Baynton basalt, black squares are the Baynton basalt weathering profile (see text for references). White circles are the Los Angeles, Shergotty, EETA79001A/B, QUE94201, SaU005, Zagami, and DaG476 basaltic Shergottites; data from compilation by *Meyer* [2004]. Gray diamonds are minerals: Hb, hornblende; Bi, biotite; Ch, chlorite; Sm, smectite; ill, illite; Ka/Gi, kaolinite and gibbsite (after *Nesbitt and Wilson* [1992]).

Tosca et al., 2005] produces alteration products that do not evolve in a similar manner to weathering profiles on Earth. Instead, the primary processes thought to control the composition of altered materials on Mars, namely acidic alteration and secondary sulfate and Fe oxide formation, produce weathering products whose chemical composition does not lend itself to comparison with terrestrial weathering products.

[4] In this paper, we present a brief overview of the primary controls on the major element chemistry of weathering profiles generated on Earth, followed by a comparison to the results of low-pH alteration experiments. These experimental results are then applied to understanding rock surface alteration profiles exposed using the Rock Abrasion Tool (RAT) [*Gorevan et al.*, 2003], and analyzed using the Alpha Particle X-ray Spectrometer (APXS) [*Rieder et al.*, 2003], onboard the Spirit rover at Gusev crater. Finally, soil chemistry from the Spirit, Opportunity, and Sojourner rovers, as well as the Viking 1 lander, are examined utilizing insights gained by the examination of rock weathering at Gusev.

2. Discussion I: The Effect of pH on Weathering Relationships

2.1. Terrestrial Weathering

[5] Figure 1 is a ternary diagram that plots the mole fractions of FeO_T + MgO, Al_2O_3, and CaO + Na_2O + K_2O at the apices. The compositions of many important primary igneous and secondary alteration minerals are plotted in Figure 1, with most of the phases having distinct locations on the diagram. This separation among phases makes this diagram particularly useful for visualizing mixing and mass balance relationships, as well as for tracking alteration pathways during weathering. These types of diagrams have been successfully utilized to predict the major element and mineralogical composition of weathering profiles generated on primary igneous rocks at the Earth's surface [*Fedo et al.*, 1995; *Nesbitt and Young*, 1982; *Nesbitt et al.*, 1996], and will be utilized throughout this paper. Plotted in Figure 1 are data for weathering profiles generated on the Baynton basalt [*Nesbitt and Wilson*, 1992] and the Toorongo granodiorite [*Nesbitt and Markovics*, 1997]. Both weathering profiles were developed in temperate climates in Australia (700–1500 mm average annual rainfall, seasonal temperature range −5°–38°C), and demonstrate the chemical and mineralogical changes that can take place as basalt and granodiorite are weathered at the Earth's surface. Also plotted in Figure 1 are a number of Martian rock compositions.

[6] As shown in Figure 1, the primary compositional variability of the various basaltic igneous rocks follows a trend subparallel to a tie line drawn between feldspar and the FeO_T + MgO apex. This is because, for the elements plotted, the basalts represent mixtures of feldspar, olivine, pyroxene, and Fe-Ti oxides. The Toorongo granodiorite represents a mixture of feldspar, biotite, amphibole, and Fe-Ti oxides. The weathering trends (shown by the arrows in Figure 1), indicate that the main consequence of weathering at the Earth's surface is to leach primary igneous minerals of the soluble elements Ca, Na, Mg, and to a lesser extent K, while enriching the weathering profile in the insoluble elements Al and Fe (in the form of Fe^{3+}). As a consequence of the leaching process, terrestrial waters become enriched in soluble elements and evolve toward the CaO + Na_2O + K_2O apex of Figure 1, while the solid products of basaltic weathering evolve in the opposite direction. As discussed below, these weathering trends develop primarily as a result of one major factor: the pH of the waters which are altering primary igneous rocks at the Earth's surface.

[7] With the exception of rare acidic regimes (e.g., hydrothermal systems, acid-saline lakes), subaerial alteration on Earth primarily occurs as rainwater percolates through the subsurface. The pH of "pristine" rainwater is buffered by carbonic acid equilibria at pH = 5.65, and is typically elevated in groundwater to near neutral pH by acid buffering reactions with minerals. In areas of high rainfall where the acid neutralizing capability of the local soil and bedrock has been exceeded (e.g., Hawaiian rain forest soils) groundwater typically has a pH of 5–6 [*Patterson*, 1971]. On the other hand, in sparsely vegetated regions of Iceland, where there is little organic matter to supply CO_2 to surface waters and form carbonic acid, the chemical alteration of basaltic glass can elevate groundwater pH to values as high as 9–10 [*Gislason and Arnorsson*, 1993]. Therefore a range of groundwater pH which encompasses conditions typically encountered in terrestrial basaltic aquifers is approximately pH = 5–9.

[8] In Figures 2a and 2b the speciation of Al and Fe^{3+} in solution is plotted on diagrams of log activity versus pH. These diagrams were calculated with the program Act2, which is part of the software package *The Geochemist's*

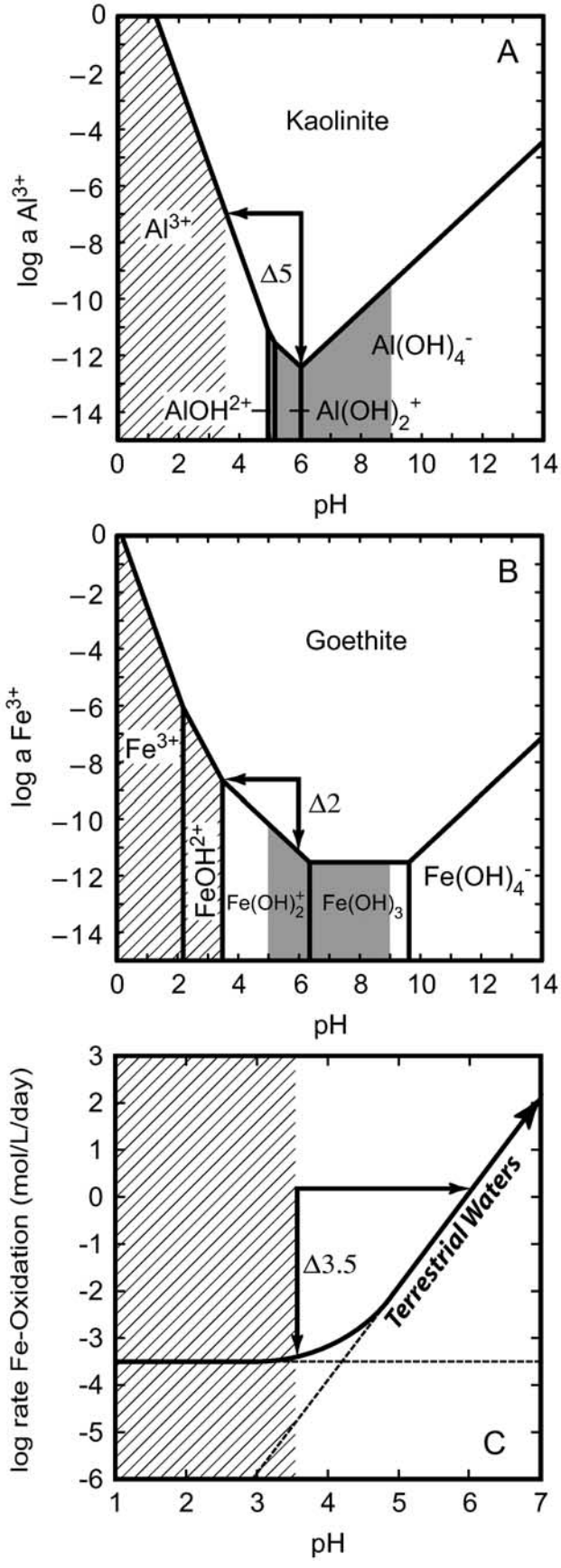

Workbench® [*Bethke*, 2002]. Similar diagrams can be calculated for other elements present in basalt (e.g., Fe^{2+}, Ca^{2+}, Mg^{2+}, K^{+}, Na^{+}), however, we have chosen not to illustrate those examples here due to the high solubility of these elements relative to Fe^{3+} and Al. As shown in Figures 2a and 2b, the pH values of most terrestrial basaltic aquifers (~5–9) fall at or near the solubility minima of Al and Fe^{3+} with respect to the secondary mineral phases kaolinite and goethite, respectively. Qualitatively similar topologies are demonstrated by generating the same types of diagrams to include other aluminum and ferric iron bearing secondary phases such as gibbsite, hematite, and $Fe(OH)_3$, which may provide additional sinks for aluminum and ferric iron. We have chosen to illustrate kaolinite and goethite as examples since these are two common secondary minerals in terrestrial weathering profiles developed on basaltic bedrock [*Gislason et al.*, 1996; *Karrat et al.*, 1998; *Nesbitt and Wilson*, 1992]. The relationships shown in Figures 2a and 2b indicate that as primary mineral dissolution occurs under normal terrestrial conditions (i.e., pH = 5–9), little Al or Fe^{3+} can be accommodated in solution before saturation with respect to secondary phases is reached. Once saturation with respect to secondary phases is attained, precipitation of those phases is thermodynamically favorable.

[9] Another important factor controlled by pH is the rate at which Fe^{2+} released to solution oxidizes to Fe^{3+} [e.g., *Burns and Fisher*, 1993]. The rate of iron oxidation increases 100-fold for every unit increase in pH at values greater than about pH = 4, whereas the rate of iron oxidation is constant for pH less than about 4, as shown in Figure 2c. As a result of this pH dependence on Fe oxidation rate, any Fe^{2+} released to solution oxidizes rapidly to insoluble Fe^{3+} under the pH conditions of most natural waters on Earth. The majority of the iron present in unaltered basaltic rocks is Fe^{2+}, which is highly soluble and readily leached from primary ferromagnesian minerals. However, due to the rapid oxidation kinetics of Fe^{2+} in terrestrial waters, most Fe^{2+} is converted to Fe^{3+} and precipitates out of solution as a ferric oxide mineral (e.g., goethite).

[10] As demonstrated by Figures 2a–2c, Al and Fe^{3+} solubility are low and the rate of Fe^{2+} oxidation is rapid in

Figure 2. (a) Log activity of Al^{3+} versus pH, showing speciation of Al with respect to kaolinite precipitation. Activity of SiO_2(aq) set by assuming saturation with respect to amorphous silica, pyrophyllite precipitation suppressed. Note that there is a 5 order of magnitude difference in Al^{3+} solubility between pH 6 and pH 3.5 (arrowheaded line with delta symbol). (b) Log activity of Fe^{3+} versus pH, showing speciation of ferric iron with respect to goethite precipitation, hematite precipitation suppressed. Note that there is a 2 order of magnitude difference in Fe^{3+} solubility between pH 6 and pH 3.5. (c) Log rate of iron oxidation (mol/L/day) versus pH. Diagram calculated at 25°C, pO_2 = 0.2 atm, and activity Fe^{2+} = 1 using rate equations of *Stumm and Morgan* [1996]. Note that there is a 3.5 order of magnitude difference in iron oxidation rate between pH 6 and pH 3.5. On all diagrams, shading denotes the pH range of most natural terrestrial waters, and the cross-hatched field represents the pH range of experiments conducted by *Hurowitz et al.* [2005] and *Tosca et al.* [2004].

Table 1. Tabulation of Data Utilized for Calculation of Altered Basalt Compositions

Oxides, wt %	LA Basalt[a]	LA Calculated Residue[b]	PFS Basalt[a]	PFS Calculated Residue[b]
SiO_2	49.0	58.0	48.7	54.9
TiO_2	1.27	0.17	1.16	1.33
Al_2O_3	10.9	0.43	10.3	12.8
FeO_T	20.4	24.5	19.2	13.2
MnO	0.43	0.68	0.49	0.34
MgO	3.34	5.82	7.66	3.59
CaO	9.7	9.67	7.07	8.61
Na_2O	2.32	0.69	3.56	4.43
K_2O	0.26	NA	0.67	0.83
Mass, g	**0.1074**	**0.05**	**0.1502**	**0.12**
Element, mol/L	LA Solution B2-10[c]		PFS Solution A (331 hrs)[c]	
Si	4.22×10^{-3}		7.91×10^{-2}	
Ti	1.63×10^{-4}		1.20×10^{-3}	
Al	2.30×10^{-3}		5.54×10^{-4}	
Fe	1.44×10^{-3}		1.21×10^{-1}	
Mn	1.93×10^{-5}		3.06×10^{-3}	
Mg	2.04×10^{-4}		1.19×10^{-1}	
Ca	1.05×10^{-3}		3.23×10^{-3}	
Na	7.07×10^{-4}		4.58×10^{-4}	
K	NA		9.31×10^{-5}	
Mass, g	**100**		**1.5**	

[a]Bulk compositions and mass of synthetic Los Angeles (LA) basalt and Pathfinder Soil (PFS) basalt from *Hurowitz et al.* [2005] and *Tosca et al.* [2004], respectively.
[b]Calculated compositions and mass of residue remaining from experimental alteration of LA and PFS basalts.
[c]Solution compositions and mass of effluent samples B2-10 and PFS Solution-A (331 hours) from *Hurowitz et al.* [2005] and *Tosca et al.* [2004], respectively.

terrestrial groundwaters. The end result of these pH-driven effects is that as alteration occurs, the Al and Fe released to solution from primary mineral dissolution tends to precipitate from solution in the form of aluminum- and ferric iron–bearing secondary minerals. The elements Mg, Ca, Na, and K, on the other hand, are leached from the weathering profile due to their relatively high solubility. This combination of precipitation and leaching results in a passive enrichment in both total Fe and Al for weathered rocks, as indicated by the weathering trends in Figure 1. If weathering on Mars were to have taken place under pH conditions similar to those on Earth, we might expect the altered rocks and soils analyzed on Mars to evolve in a geochemically similar manner, with the altered materials being enriched in total Fe and Al relative to the unaltered igneous rocks from which they are derived.

[11] We note that the calculations used to generate Figure 2a only include aqueous Al^{3+}, SiO_2, and H^+. Similarly, for Figure 2b only Fe^{3+} and H^+ are included. The equilibrium solubility relationships for these elements will undoubtedly become more complex as more aqueous species are included in the calculations. For example, different phyllosilicate minerals would be predicted to precipitate if other cations (e.g., K^+, Na^+, Ca^{2+}) were included in the calculations for Figure 2a. Similarly, Fe^{3+} solubility could increase by the inclusion of SO_4^{2-} in the calculations for Figure 2b. For the purposes of simplicity, we have chosen to show straightforward scenarios in Figures 2a and 2b to illustrate the basic point that Al^{3+} and Fe^{3+} solubility are controlled by pH.

2.2. Experimental Weathering at Low pH

[12] It is generally accepted that the high concentrations of S and Cl in Martian soils are consistent with the presence of a salt component which numerous authors have suggested formed in a low-pH environment rich in acidic sulfate and chloride species [e.g., *Burns*, 1987; *Clark and Van Hart*, 1981; *Newsom et al.*, 1999]. This salt component appears to be a ubiquitous feature of soils and rocks analyzed at widely separated geographical locations on the Martian surface [*Clark et al.*, 1982; *Foley et al.*, 2003; *Gellert et al.*, 2004; *Rieder et al.*, 2004]. This had led some early workers to propose that aqueous fluids are dominantly acidic in the Martian surface and shallow subsurface [*Banin et al.*, 1997; *Burns*, 1993; *Burns and Fisher*, 1993; *Settle*, 1979]. Recently, direct evidence for the presence of acidic groundwater systems in the Martian near-surface environment has been provided by the identification of jarosite at the Opportunity landing site [*Klingelhöfer et al.*, 2004; *Squyres et al.*, 2004; *Tosca et al.*, 2005], Fe^{3+} sulfate in soils of the Columbia Hills [*Morris et al.*, 2006], and the possible presence of polyhydrated Fe-Al sulfates such as copiapite and halotrichite in layered deposits in Valles Marineris and Meridiani Terra [*Gendrin et al.*, 2005].

[13] In experimental studies by *Hurowitz et al.* [2005] and *Tosca et al.* [2004], synthetic basalts of Martian composition were experimentally altered under low-pH conditions (pH $\sim$ 0–3.5) in order to ascertain the nature of the secondary minerals produced by alteration of Martian basalts in acidic environments. In both studies, experiments were performed in which basalts of Martian composition were synthesized and then altered in batch and flow-through reactors under variable conditions of pH and water-to-rock ratio. The unaltered basalts were characterized by electron microprobe (EMP) and X-ray diffraction (XRD). During the course of alteration, fluid compositions were analyzed by direct current plasma argon emission spectroscopy (DCP). Following alteration, basaltic residues and secondary phases were analyzed by a combination of XRD, scanning electron microscopy, and Raman spectroscopy.

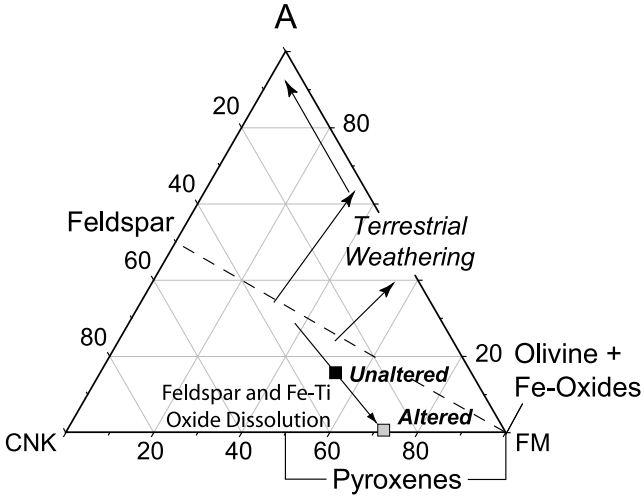

Figure 3. Ternary diagram showing the composition of the synthetic Los Angeles Shergottite basalt (LA) (black square) [*Hurowitz et al.*, 2005] and calculated residue (shaded square) remaining after alteration at pH = 1.0 and water to rock ratio = 1000. As shown, alteration is dominated by dissolution of plagioclase. Note, however, that the plagioclase dissolution trend does not extend to the position of plagioclase, indicating that the dissolution of titanomagnetite also plays a role in determining the dissolution trend vector as well. Also shown are the terrestrial weathering trends from Figure 1.

[14] Because the quantitative chemical compositions of the altered basalts were not measured directly in either *Tosca et al.* [2004] or *Hurowitz et al.* [2005], we have calculated the bulk chemical compositions of the altered basalts produced during low-pH experimentation using the composition of the starting basalt (as determined by EMP) and the fluid compositions produced during alteration (as determined by DCP). The results of these calculations are shown in Table 1 and Figures 3 and 4. We emphasize the results of the lowest pH and highest water to rock ratio experiments from these two studies because they generate the largest differences in chemical composition between primary basalt and altered residue. These calculated residual compositions reveal the nature of chemical fractionations produced during low-pH alteration in much the same way that the Baynton basalt and Toorongo granodiorite weathering profiles do for terrestrial weathering (Figure 1).

[15] From the results of *Hurowitz et al.* [2005], data for the alteration of an olivine-free synthetic Los Angeles basaltic shergottite at pH = 1.0 and water to rock ratio = 1000 is shown in Figure 3. As discussed in their study, dissolution of the primary mineral phases labradorite and titanomagnetite dominates the solution chemistry, and as a result, the calculated residual basalt becomes depleted in Al, Na, Ti, and Ca. Owing to its slow dissolution rate relative to labradorite and titanomagnetite under these conditions, clinopyroxene remained relatively unaltered in the experiments. Not surprisingly then, the calculated composition of the altered residue evolves toward a composition resembling that of pyroxene by removal of the elements associated with plagioclase and titanomagnetite (Figure 3). The calculated mass loss from the original basalt is ~50% (Table 1), with the lost mass going into the formation of secondary phases, predominantly sulfates and amorphous silica [*Hurowitz et al.*, 2005].

[16] From the results of *Tosca et al.* [2004], data for the alteration (pH = 0, water to rock ratio = 10) of an olivine-bearing synthetic basalt having a composition based on S- and Cl-free Pathfinder soil analyses is shown in Figure 4 (see *Tosca et al.* [2004] for a discussion of this composition). As discussed in that study, the dissolution of the primary mineral phase olivine dominates the solution chemistry, and as a result, the calculated residual basalt becomes depleted in Mg and Fe. The calculated mass loss from the original basalt is ~20% (Table 1); again, the lost mass goes into the formation of secondary phases, predominantly sulfates and amorphous silica [*Tosca et al.*, 2004].

[17] It is clear from inspection of Figures 3 and 4 that alteration at low pH results in vastly different weathering trends than those observed for alteration under typical terrestrial conditions (compare to terrestrial weathering trends shown in Figures 1, 3, and 4). In large part, these differences result from the fact that Al and Fe^{3+} are orders of magnitude more soluble under the low-pH experimental conditions of *Tosca et al.* [2004] and *Hurowitz et al.* [2005] than they are at the near neutral pH conditions of groundwaters on Earth (Figures 2a and 2b). In addition, the rate of Fe^{2+} oxidation is orders of magnitude lower under experimental conditions, allowing highly soluble Fe^{2+} to remain in solution without oxidizing to less soluble Fe^{3+} for a longer time period (Figure 2c). These pH driven effects allow dissolved Al and Fe to remain in solution at much higher concentrations than at the near-neutral pH conditions of terrestrial waters. As a result, the experimentally altered basalts do not become passively enriched in

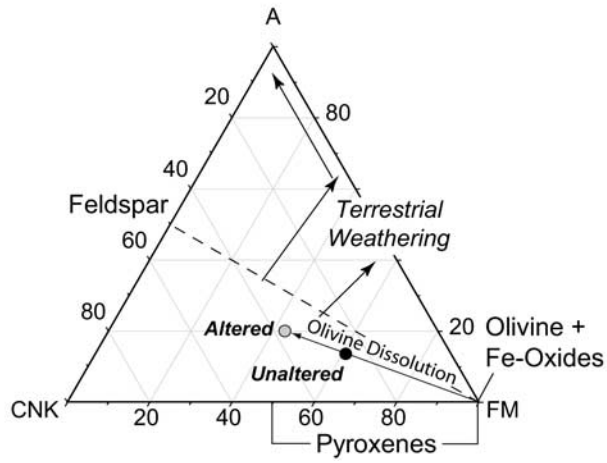

Figure 4. Ternary diagram showing the composition of the synthetic Pathfinder soil basalt (PFS) (black circle) [*Tosca et al.*, 2004] and calculated residue (shaded circle) remaining after alteration at pH = 0 and water to rock ratio = 10. As shown, alteration is dominated by dissolution of olivine.

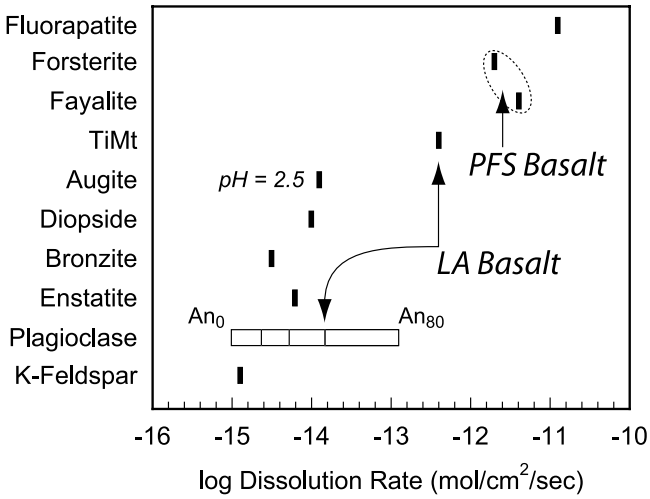

Figure 5. Log mineral dissolution rates (mol/cm^2/sec) determined experimentally at pH = 2 and 25°C. Data from *Blum and Stillings* [1995], *Brantley and Chen* [1995], *Guidry and Mackenzie* [2003], *Pokrovsky and Schott* [2000], *White et al.* [1994], and *Wogelius and Walther* [1992]. Arrows point to fastest dissolving mineral phases present in synthetic LA and PFS basalts [*Hurowitz et al.*, 2005; *Tosca et al.*, 2004]; see text for details.

aluminum or iron as naturally weathered basalts do on Earth.

[18] From the experimental data it is apparent that at low pH, basaltic residues simply become depleted in the elements contained in the primary minerals undergoing the most rapid alteration. Accordingly, the relative dissolution rates of the minerals undergoing alteration will determine which mineral(s) exert the greatest control on solution chemistry and basaltic residue composition. Plotted in Figure 5 are the experimentally determined dissolution rates (pH = 2, 25°C) of some primary igneous mineral phases. For the olivine-free Los Angeles basalt, the two primary phases with the fastest dissolution rate are titanomagnetite and labradorite, and both solution composition and residual basalt compositions are controlled by the dissolution of these phases (Figure 3). The same effect is seen for the olivine bearing basalt composition of *Tosca et al.* [2004], in which the fastest dissolving phase is olivine (Figure 4). This is not to say that only labradorite and titanomagnetite are dissolving from the Los Angeles basalt, and that only olivine is dissolving from the olivine-bearing basalt composition, as all of the phases in the basalt are undergoing dissolution. The acid dissolution process is not selective for one mineral versus another, but the fluid chemistry is dominated by input from the phase, or phases, that alter the most rapidly. This is an important point for later discussion of rock alteration trends at Gusev, whose geochemistry is also dominated by the dissolution of the most readily altered phases.

[19] Another interesting effect of low-pH alteration is that the trends shown for the dissolution of olivine-free and olivine-bearing basalts (Figures 3 and 4) are subparallel to the primary compositional variability of unaltered igneous rocks (Figure 1). This may make the effects of weathering in a low-pH environment difficult to distinguish from simple compositional heterogeneity among unaltered rocks and soils. However, as will be discussed below, the differences between rock surface and rock interior chemistry (as revealed by the RAT) can be understood in terms of the low-pH dissolution relationships just discussed.

2.3. Water to Rock Ratio and the Evolution of Solution pH

[20] The terrestrial and experimental cases presented above can be thought of as two extremes on a continuum of chemical changes which will be caused by the interaction between water and rock. In the terrestrial case, the changes in bulk chemical composition occurring during alteration have taken place as a result of interaction between moderate pH water and basalt at high water to rock ratio. In the experimental case, the changes brought about by alteration have occurred by interaction between extremely acidic waters and basalt at variable water to rock ratio. In the experimental cases presented, the fluids were acidic enough that little, if any, change in solution pH occurred as a result of interaction between solution and basalt. The experiments were of relatively short duration, and the alteration process was effectively halted by evaporation of the fluids following a set period in which alteration was allowed to occur. While this scenario may appear somewhat unusual from a terrestrial standpoint, the changes in rock surface chemistry apparent for rocks analyzed by the Spirit rover at Gusev

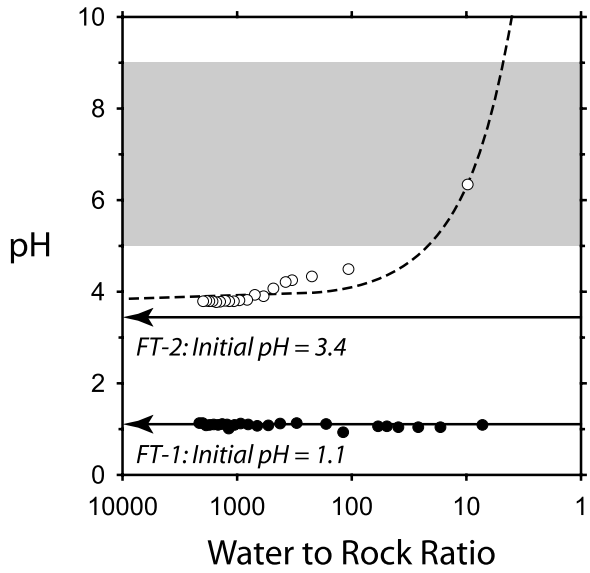

Figure 6. pH versus water to rock ratio showing data from the flow-through experiments FT-1 and FT-2 of *Hurowitz et al.* [2005]. Solid arrowheaded lines show the initial pH of the system at the beginning of each experiment and indicate the direction of reaction progress from experiment start to completion. The dashed line is a first-order polynomial fit to the data for experiment FT-2. Shaded field denotes pH range = 5–9, typical of terrestrial basaltic aquifers. The initial pH of experiment FT-1 is unmodified over the course of the experiment, whereas the initial pH of experiment FT-2 is significantly elevated at low water to rock ratio by acid neutralization reactions between the fluid and basalt.

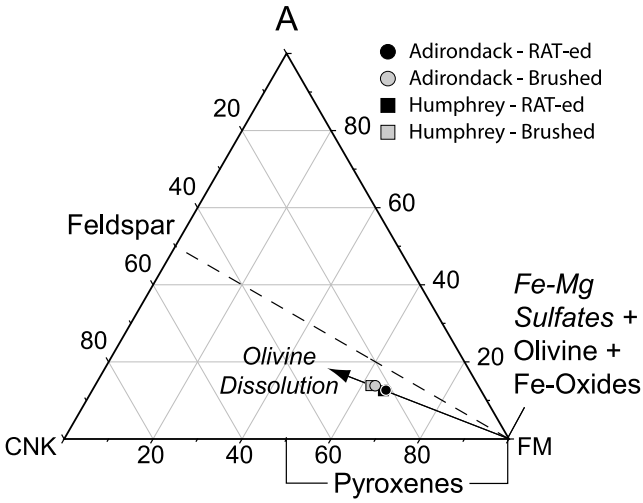

Figure 7. Ternary diagram showing the composition of target Adirondack_RAT (black circle with white outline), Adirondack_brush (shaded circle), Humphrey_RAT2 (black square), and Humphrey_brush (shaded square). Data from *Gellert et al.* [2006] and *Rieder* [2004]. The brushed analyses are depleted in FeO_T and MgO relative to RATted analyses, indicating dissolution of olivine from the rock surfaces.

crater are well described by the experimental data (as will be discussed below).

[21] It is important to recognize that interaction between acidic fluids and basalt should result in the eventual neutralization of pH via the exchange of H^+ from solution for cations present in the basalt. The degree to which solutions are neutralized by such reactions will be largely dependent on the initial pH of the solution in contact with basalt and the water to rock ratio. We can illustrate this point by way of a simple example, utilizing data from flow-through alteration experiments on synthetic Los Angeles basalt conducted at two different initial pH values: 1.1 and 3.4 [*Hurowitz et al.*, 2005]. As shown in Figure 6, for the case of initial pH = 1.1, the solution pH remains very acidic over a wide range of water to rock ratio (∼2000 to ∼10). This solution has such a high concentration of H^+, that there is insufficient basalt in the system to modify the solution pH, even at low water to rock ratio. In the second case (initial pH = 3.4), the pH was elevated to near-neutral at the beginning of the experiment, and as more fluid was passed over the basalt (i.e., water to rock ratio was increased), the pH of the solution returned to values close to the initial value. What these examples indicate is that, except at very low water to rock ratio, pH will generally remain acidic provided the initial pH of the system is low enough. As the initial pH of the system increases, the amount of rock required to elevate pH to values near neutral will be lower.

[22] In a general sense, we can conclude that as the initial pH of the solution in contact with basalt increases, one should still expect to see qualitatively similar changes in bulk rock chemical composition to those shown in Table 1 and Figures 3 and 4, provided that the solution pH remains below about pH = 4. Under such conditions the solubility of Al and Fe^{3+} are substantially higher than that seen for the circumneutral pH typical of terrestrial alteration (Figures 2a and 2b), and there should be no change in the behavior of Fe^{2+} leached from basalt since the rate of Fe oxidation is pH-independent in this range (Figure 2c). Therefore under such conditions the passive Fe and Al enrichment common to terrestrial weathering profiles (Figure 1), which results from the insolubility of Al and Fe^{3+} and the rapid oxidation of Fe^{2+} to insoluble Fe^{3+} phases, should not be observed. However, as the examples in Figure 6 illustrate, as initial pH increases, more fluid will be required in order to maintain the low-pH conditions under which the experimental alteration trends shown in Figures 3 and 4 are valid. In addition, as initial pH increases, more fluid will be required in order to generate large changes in rock chemistry since mineral dissolution rates decrease as pH increases [*White and Brantley*, 1995]. Clearly, the details of exactly how the alteration trends shown in Figures 3 and 4 evolve from the acidic pH regime (pH ∼ 0–4) to the mildly acidic/neutral pH regime (pH ∼ 4–7), is an area which requires further systematic experimental investigation.

3. Discussion II: Application to Martian Rocks and Soils

3.1. Rock Analyses

[23] APXS analyses of rocks will be discussed in terms of "Surface," "Brushed," and "RATted" analyses. These represent analyses of pristine rock surfaces ("Surface"), rock surfaces which have had adhering soil and dust removed by the RAT brush ("Brushed"), and rocks which have been ground to variable depth by the RAT ("RATted"). Microscopic Imager (MI) views of brushed and RATted surfaces on the rock "Humphrey" can be found in *Arvidson et al.* [2006, Figure 11], and MI views of surface, brushed, and RATted surfaces on the rock "Adirondack" can be found in *Herkenhoff et al.* [2004, Figure 4]. As discussed by S. P. Gorevan et al. (Rock Abrasion Tool: Mars Exploration Rover mission, manuscript in preparation, 2006), in order to remove adhering fines from rock surfaces the RAT uses its Rotate Brush to sweep a 45 mm diameter spot of zero depth at the rock surface. The RAT then uses its grinding wheel to grind a 45 mm diameter hole with a nominal depth of 5 mm into the rock. The actual depth of RAT grinds into rocks analyzed at Gusev ranged from approximately 2 to 9 mm, and RAT grind depths are tabulated on a rock-by-rock basis by *Arvidson et al.* [2006]. A summary of rock analysis operations organized by sol number can also be found in *Arvidson et al.* [2006].

3.2. Adirondack Class Basalts

[24] As discussed by *McSween et al.* [2004] the RATted rocks analyzed on the Gusev Plains (Adirondack, Humphrey, Mazatzal) are olivine-normative picritic basalts. These rocks are part of the "Adirondack Class" of basalts [*Squyres et al.*, 2006]. The rocks Adirondack and Humphrey are discussed below. The rock Mazatzal is not discussed in this report due to the presence of a thick and complex coating [*Haskin et al.*, 2005; *Morris et al.*, 2004] which obscures the low-pH dissolution relationships evident for Adirondack and Humphrey.

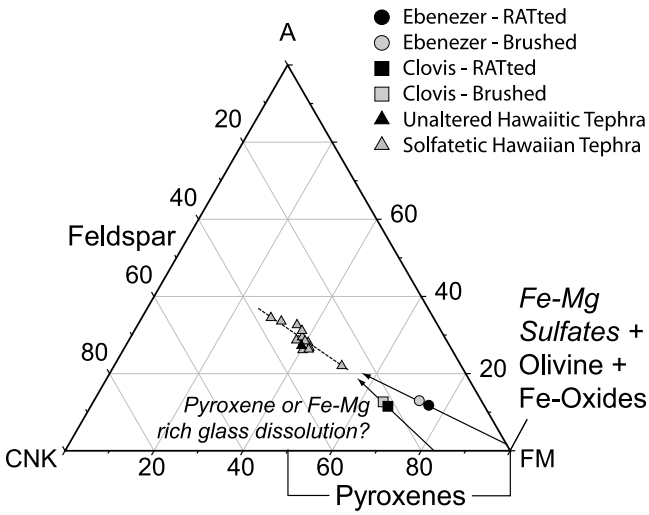

Figure 8. Ternary diagram showing the composition of target Ebenezer_RAT (black circle), Ebenezer_brushed (shaded circle), Clovis_Plano_RAT (black square), and Clovis_Plano_Brush (shaded square). Data from *Gellert et al.* [2006] and *Rieder* [2004]. The brushed analyses of Ebenezer and Clovis are depleted in FeO_T and MgO relative to RATted analyses, possibly indicating dissolution of pyroxene and/or basaltic glass from the rock surfaces. Also shown are the average unaltered Hawaiitic tephra (black triangle) and solfatetic tephras (shaded triangles) of *Morris et al.* [2000].

[25] Data for the brushed and RATted surfaces of Adirondack and Humphrey are shown in Figure 7. In this, and all subsequent ternary plots discussed in this paper, the symbols occupy a space on the diagrams representing approximately ±1.0% in "ternary space." Analytical uncertainties for the individual elements plotted are highly variable (from 0.5 to 72% relative). However, when recalculated and plotted on ternary diagrams, the cumulative uncertainties rarely constitute more than ±1.0% (i.e., the error bars lie within the space occupied by the symbols). For analyses which have uncertainty >1.0%, error bars have been plotted, for all others, no error bars are shown.

[26] As shown in Figure 7, the brushed rock surfaces of Adirondack and Humphrey are depleted in MgO and FeO_T relative to the RATted rock interiors. These relationships indicate that the difference between the RATted and brushed compositions could plausibly be interpreted as resulting from dissolution of olivine at the rock surface. Note the similarity to the experimental dissolution trend shown in Figure 4. In both of the above cases (Adirondack, Humphrey), the small offsets in ternary space between brushed and RATted surfaces indicate a low degree of alteration. The offset between these data points is significantly smaller than that shown for the experimental alteration of olivine-bearing basalt (Figure 4), indicating that if alteration of the Adirondack class basalts also took place at pH = 0, then either the water to rock ratio was <10, or the cumulative duration of alteration was shorter than 2 weeks. These are the water to rock ratio and time period, respectively, over which alteration experiments were conducted. For less aggressive initial pH conditions, higher water to rock ratios (and/or longer-duration alteration events) are possible. The small offsets between RATted and brushed analyses, however, appear to indicate limited interaction between fluid and basalt.

[27] The Mössbauer data from the brushed and RATted surfaces of both rocks are consistent with the olivine dissolution trend apparent from the APXS data. Assuming that the composition of the olivine does not change between brushed and RATted surfaces, the values obtained by multiplying the olivine abundance derived from Mössbauer by the FeO_T content from APXS indicates that the amount of iron associated with olivine decreases from the brushed to RATted surfaces of Adirondack and Humphrey [*Gellert et al.*, 2006; *Klingelhöfer*, 2004; *Morris et al.*, 2004; *Rieder*, 2004]. It is important to note, however, that caution is warranted in combining Mössbauer and APXS data because their respective radiation sources have different penetration depths [*Klingelhöfer et al.*, 2003; *Rieder et al.*, 2003].

3.3. Clovis Class Rocks

[28] The RATted rocks analyzed at the West Spur region of Husband Hill (Clovis, Ebenezer) are part of the "Clovis Class" of rocks [*Squyres et al.*, 2006]. For a thorough discussion of the possible origins of these rocks, see *Ming et al.* [2006], *Morris et al.* [2006], and *Squyres et al.* [2006], who interpret these rocks to be more pervasively altered rocks than the Adirondack class basalts. From the standpoint of Mössbauer spectroscopy, these rocks are highly oxidized, characterized primarily by abundant Fe oxides and lesser pyroxene (~12–15% of Mössbauer component area), and only trace olivine (~1% of Mössbauer component area) [*Klingelhöfer*, 2004; *Morris et al.*, 2006].

[29] In Figure 8, the data for the brushed and RATted surfaces of Clovis and Ebenezer are shown. Similar to the Adirondack class basalts, the brushed rock surfaces of Clovis and Ebenezer are depleted in MgO and FeO_T relative to the RATted rock interiors, with relatively small offsets between brushed and RATted analyses. These relationships indicate that the brushed surfaces of these rocks have undergone the same type of surface alteration process as the Adirondack class basalts, resulting in the loss of an Fe-Mg rich phase. In this case, Mössbauer spectroscopy does not indicate the presence of significant olivine, so this is probably not the phase controlling the apparent loss of MgO and FeO_T from the rock surface. The Mössbauer spectrometer does indicate the presence of pyroxene in these rocks and dissolution of pyroxene results in an alteration trend similar to that of the olivine dissolution trend (see Figure 8). Making the same assumptions about mineral composition discussed for the Adirondack class basalts, the amount of iron associated with pyroxene decreases slightly from the brushed to RATted surfaces of Clovis, consistent with pyroxene dissolution. No brushed rock Mössbauer analysis was made on the rock Ebenezer.

[30] Another possibility is that the observed trends result from alteration of basaltic glass. As shown in Figure 8, alteration of glassy basaltic tephras in acidic environments in Hawaii (solfatetic tephras of *Morris et al.* [2000]) results in alteration trends similar to those observed for the Clovis class rocks. Supporting such an interpretation, deconvolu-

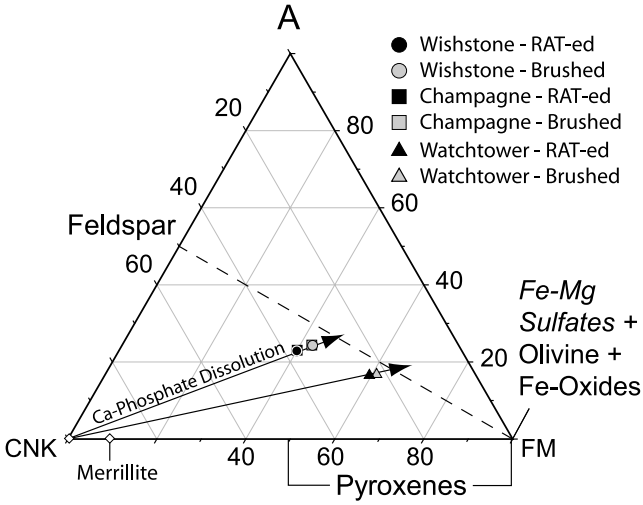

Figure 9. Ternary diagram showing the composition of Wishstone_Chisel_RAT (black circle with white outline), Wishstone_Chisel_brushed (shaded circle), Champagne_RAT (black square), Champagne_brush (shaded square), Watchtower_Joker_RAT (black triangle), and Watchtower_Joker_Brush (shaded triangle). Data from *Gellert et al.* [2006] and *Rieder* [2004]. Also plotted is Na-merrillite ($Ca_{18}Na_2Mg_2(PO_4)_{14}$, white diamond). The brushed analyses are depleted in CaO relative to RATted analyses, indicating dissolution of Ca-phosphate from the rock surfaces.

tion of miniature thermal emission spectrometer (MiniTES) spectra from rocks of the West Spur region indicates a high abundance of a short-order aluminosilicate phase (S. W. Ruff et al., The rocks of Gusev crater as viewed by the Mini-TES instrument, manuscript in preparation, 2006; hereinafter referred to as Ruff et al., manuscript in preparation, 2006). This identification could be indicative of fresh basaltic glass and/or a poorly crystalline alteration phase (such as allophane) which could be derived from the weathering of basaltic glass [*Michalski et al.*, 2005a, 2005b; Ruff et al., manuscript in preparation, 2006].

3.4. Wishstone and Watchtower Class Rocks

[31] The RATted rocks Champagne and Wishstone analyzed during the traverse between the West Spur and Cumberland Ridge regions of Husband Hill are collectively known as "Wishstone Class" rocks [*Squyres et al.*, 2006]. The rock Watchtower is the only one of its class (Watchtower Class) to have both brushed and RATted analyses, and it will be discussed in this section as well. As discussed by *Arvidson et al.* [2006], Champagne and Wishstone are not in-place outcrops, but Watchtower is an outcrop. These two rock classes differ in a number of important aspects including FeO_T, MgO, and SO_3 concentrations, Fe mineralogy, and Fe oxidation state [*Gellert et al.*, 2006; *Klingelhöfer*, 2004; *Morris et al.*, 2006; *Rieder*, 2004; *Squyres et al.*, 2006]. However, both rock types are similar in that they are characterized by Cr_2O_3 concentrations which are below the APXS detection limit, high concentrations of TiO_2 (2.21–2.96 wt %) and high concentrations of P_2O_5 (4.7–5.5 wt %) with a strong positive correlation between P_2O_5 and CaO, suggesting that the P_2O_5 is present as a Ca-phosphate phase [*Ming et al.*, 2006]. In addition, both rock types appear to be affected by a similar rock surface alteration process, and for this reason, these two rocks types are grouped together in the following discussion.

[32] In Figure 9, the data for the brushed and RATted surfaces of Champagne, Wishstone and Watchtower are shown. The brushed surfaces of all three rocks are depleted in CaO relative to corresponding RATted surfaces. Assuming that much of the CaO in these rocks is present as a phosphatic phase, the depletion of CaO could be due to dissolution of a Ca-phosphate mineral. Different Ca-phosphate phases (e.g., apatites, merrillites) cannot be readily distinguished in Figure 9, as they all plot at or near the CaO apex of the diagram.

[33] In order to ascertain the nature of the phosphatic phase being removed from these rock surfaces, the brushed and RATted data points have been plotted in Figure 10, a ternary diagram which plots the mole fractions of CaO, P_2O_5, and the sum of MgO, FeO_T, Na_2O, and K_2O at the apices. In Figure 10, all of the primary igneous phases plot along the bottom of the ternary, while various Ca-phosphates plot along the CaO-P_2O_5 join. As shown, the brushed surfaces are depleted in CaO and P_2O_5 relative to the RATted surfaces, and the depletion is consistent with the removal of a phosphate mineral having a higher P_2O_5: CaO ratio than apatite,

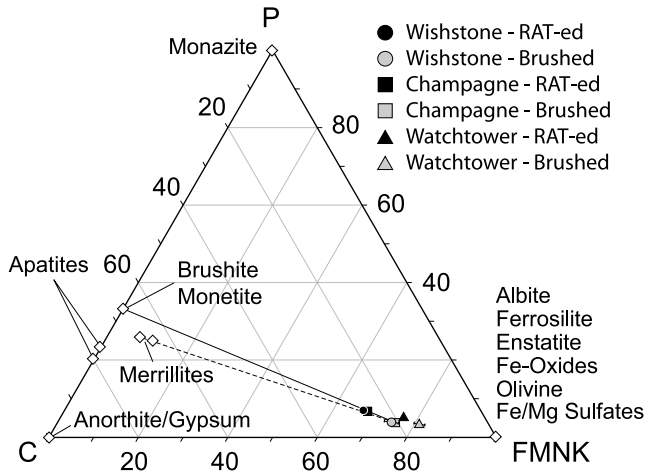

Figure 10. Ternary $FeO_T + MgO + Na_2O + K_2O$ (FMNK), P_2O_5 (P), CaO (C) diagram, data plotted in mole percent. Minerals plotted as white diamonds, formulas for apatite, carbonate apatite, Ca and Na-merrilite, brushite, and monetite are: $Ca_5(PO_4)_3(OH)_{0.33}F_{0.33}Cl_{0.33}$, $Ca_5(PO_4,CO_3)_3F$, $Ca_{19}Mg_2(PO_4)_{14}$, and $Ca_{18}Na_2Mg_2(PO_4)_{14}$, $CaHPO_4{\cdot}2H_2O$, and $CaHPO_4$, respectively. All other symbols are the same as Figure 9; data from *Gellert et al.* [2006] and *Rieder* [2004]. The solid line is an extrapolation to the CaO-P_2O_5 join of a tie line drawn between the RATted and brushed compositions of Champagne. The dashed line is drawn from the position of merrillite to the brushed composition of Champagne. It is difficult to tell which phase, brushite or merrillite, is being dissolved from the rock surface to generate the differences in chemistry between RATted and brushed analyses.

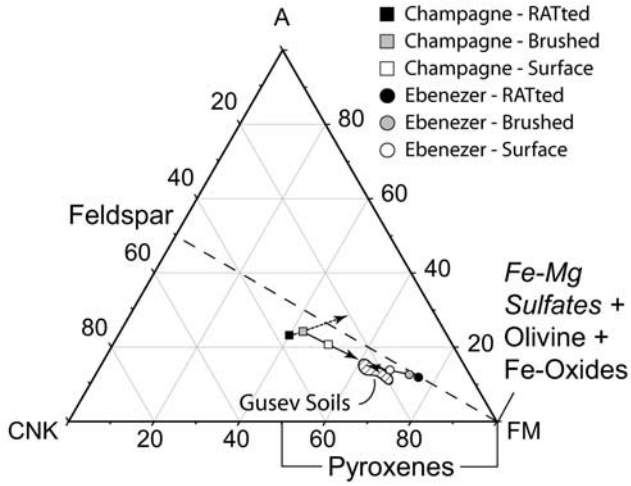

Figure 11. Ternary diagram showing the composition of Champagne_RAT (black square), Champagne_brush (shaded square), Champagne_as is (white square), Ebenezer_RAT (black circle), Ebenezer_brushed (shaded circle), and Ebenezer_as is (white circle). Also shown as a cross-hatched field are the soil analyses from Gusev crater. Data from *Gellert et al.* [2006] and *Rieder* [2004]. The dashed line is an extrapolation of a tie line between the "RATted" and "Brushed" APXS analyses of Champagne demonstrating the previously discussed mineral dissolution relationships (Figure 9). The pristine surfaces of Champagne and Ebenezer demonstrate the effect of soil addition to brushed rock surfaces, shown by the solid arrowhead lines.

possibly phases such as monetite, brushite, or merrillite. Monetite and brushite are commonly formed by precipitation from acidic, phosphorous-rich solutions [*Fiore and Laviano*, 1991; *Shellis et al.*, 1997], whereas merrillite is an igneous phosphate, actually the most common phosphatic mineral found in the SNC meteorites [*McSween and Treiman*, 1998]. Because there is not a great deal of variability in the P_2O_5: CaO ratio of these mineral phases, it is difficult to unequivocally identify the phosphate mineral present in these rocks. It is clear, however, that the differences in chemistry between brushed and RATted rock surfaces require the removal of a phosphate mineral with a higher P_2O_5: CaO ratio than apatite, which is the most common phosphate mineral encountered on Earth [*Kohn et al.*, 2002].

[34] There is little data available for the dissolution kinetics of the mineral phases monetite, brushite, or merrilite. *Tang et al.* [2003] report that brushite dissolution at pH 5.5 and 37°C is approximately 3–4 orders magnitude faster than that of apatite. *Guidry and Mackenzie* [2003] report a log dissolution rate for igneous fluorapatite at pH 2 and 25°C of -10.91 mol m^{-2} s^{-1}, which is faster than that of olivine at the same conditions (see Figure 5). We generalize on the basis of these limited dissolution rate data that phosphatic minerals may tend to dissolve more rapidly at low pH than olivine. If this is indeed the case, then it is perhaps not surprising that a phosphatic mineral present in as large quantities as indicated for the Wishstone and Watchtower class rocks would dominate the surface dissolution behavior of these rocks, even in the presence of olivine, which constitutes between ~5–20% of the Mössbauer component area of these rocks [*Klingelhöfer*, 2004; *Morris et al.*, 2006]. In much the same way that the alteration of ferromagnesian minerals likely results in the formation of secondary sulfates and iron oxides in soils, the phosphate removed from Wishstone and Watchtower class rock surfaces may be transported away from the rock surfaces and enrich local soil materials in phosphatic minerals. For example, the Paso Robles soil encountered on Husband Hill is highly enriched in phosphorous, having a P_2O_5 content of ~5.5 wt % [*Gellert et al.*, 2006; *Rieder*, 2004].

3.5. Soil Addition to Rock Surfaces

[35] The "Surface," "Brushed," and "RATted" analyses of Champagne are plotted in Figure 11. For the rocks Wishstone and Watchtower no surface APXS analysis was collected, and so these rocks are not plotted in Figure 11. As shown, the position of the surface analysis of Champagne is consistent with a two-component mixture between the brushed (altered) surface of the Champagne rock and Gusev soil. The Champagne sample illustrates another process which may be influencing APXS analyses of rock surfaces: the addition of soil and/or dust to altered rock surfaces. The Clovis class rock Ebenezer shows sample to sample variations consistent with those demonstrated by Champagne, though mixing between soils and the RATted interior of this rock cannot be unequivocally ruled out on the basis of the relationships shown in Figure 11. For the remaining rock samples discussed previously (Adirondack, Humphrey, Clovis) the RATted, brushed, and surface analyses all plot within the field of Martian soils, making distinction between soil addition to brushed surfaces versus RATted surfaces difficult.

[36] In order to further ascertain the extent to which surface APXS analyses of rocks are affected by soil addition, the surface, brushed and RATted analyses of Adirondack and Wishstone have been plotted in Figure 12a, and Humphrey, Clovis, and Ebenezer have been plotted in Figure 12b. Figures 12a and 12b are ternary diagrams which plot the mole fractions of CaO + MgO, SO_3, and Al_2O_3 at their apices. On these diagrams, the mineral dissolution relationships discussed previously result in trends directed away from the CaO+MgO apex, toward the Al_2O_3 axis. Addition of sulfate results in trends directed toward the SO_3 apex.

[37] The surface analyses of the rocks Wishstone and Adirondack (Figure 12a) clearly demonstrate a two-component mixing relationship between the brushed rock surface and Gusev soils. The mineral dissolution relationships discussed previously for brushed and RATted rock surfaces are also well demonstrated in Figure 12a, as the brushed surfaces are depleted in CaO and MgO relative to RATted surfaces. In Figure 12b, the rocks Humphrey and Clovis demonstrate surface-brushed-RATted rock relationships consistent with those shown for Adirondack and Wishstone, however, neither the Humphrey nor Clovis surface analyses appear to be as strongly affected by soil addition as the Adirondack and Wishstone surface analyses. Finally, for the Ebenezer analyses the processes of mineral

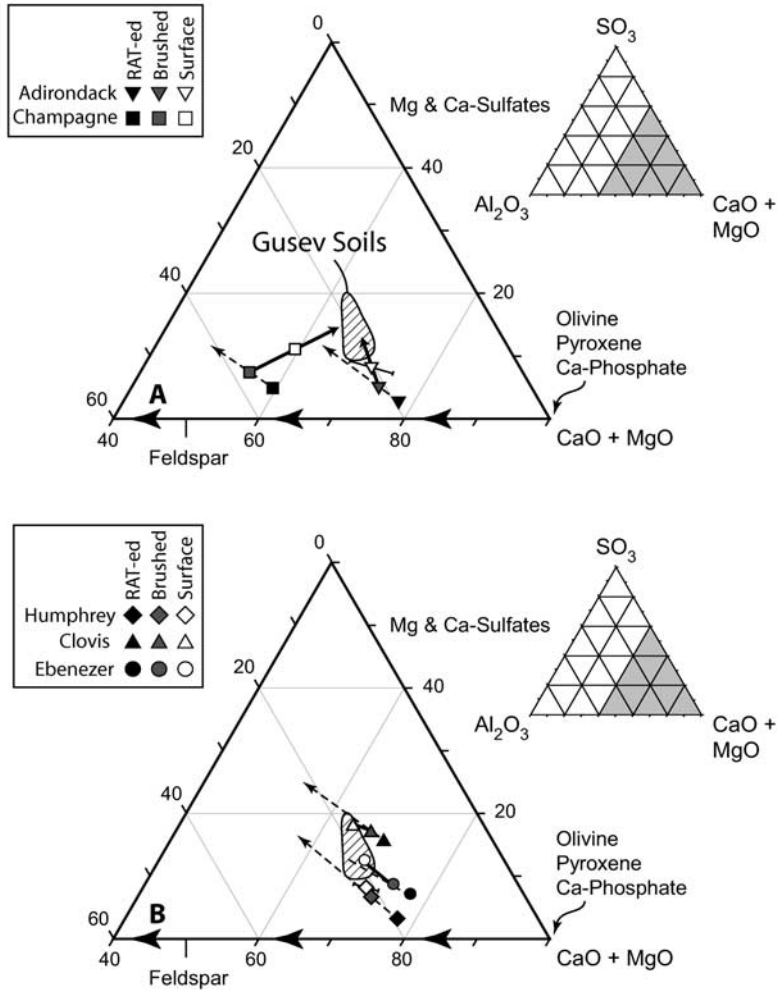

Figure 12. Ternary CaO + MgO, SO_3, Al_2O_3 diagrams, data plotted in mole percent. Only the lower right portion of the full ternary diagrams are shown, as indicated by the shaded field in the ''guide diagram'' shown on the upper right. This is done in order to magnify the differences between analyses of different rock surfaces. Figures 12a and 12b plot all Gusev soils, except subsurface soils from the ''Big Hole'' and ''The Boroughs'' trenches. The soil analysis ''Paso Robles'' plots off of both diagrams toward the SO_3 axis. Figure 12a plots the ''Surface,'' ''Brushed,'' and ''RATted'' analyses of Adirondack and Wishstone, and Figure 12b plots the same data for Humphrey, Clovis, and Ebenezer, as indicated in the legends. The dashed lines are extrapolations of tie lines between the ''RATted'' and ''Brushed'' APXS analyses and demonstrate the effect of mineral dissolution from the rock surface. The bold lines are extrapolated tie lines between the ''Brushed'' and ''Surface'' APXS analyses and demonstrate the effect of soil addition to brushed rock surfaces. The large arrowheads along the bases of both figures illustrate the effect of pure mineral phase dissolution with no addition of SO_3. All data from *Gellert et al.* [2006] and *Rieder* [2004].

dissolution at the rock surface and soil addition to the rock surface cannot be distinguished from one another since vectors from the RATted rock interior through either the brushed analysis or the surface analysis go through the field defined by Gusev soils.

[38] Figures 12a and 12b confirm that mineral dissolution at the rock surface, rather than soil addition to the rock surface, controls the differences in chemistry between RATted and brushed rock analyses. This is well demonstrated by the Adirondack class basalts, Clovis, and Wishstone. Furthermore, the process of soil addition to brushed rock surfaces appears to influence the chemistry of APXS surface analyses to a variable degree, with Adirondack and Wishstone surface analyses strongly influenced, and Humphrey and Clovis surface analyses less so. For the rock Ebenezer, the processes of mineral dissolution and soil addition cannot be distinguished unambiguously in Figure 11 or 12b, but the trends for this rock are entirely consistent with the processes described for the other rock samples. We note that these mineral dissolution and soil addition relationships may have important implications for the understanding of Pathfinder rock chemical analyses, which have been interpreted as possibly representing a mixture between unaltered igneous

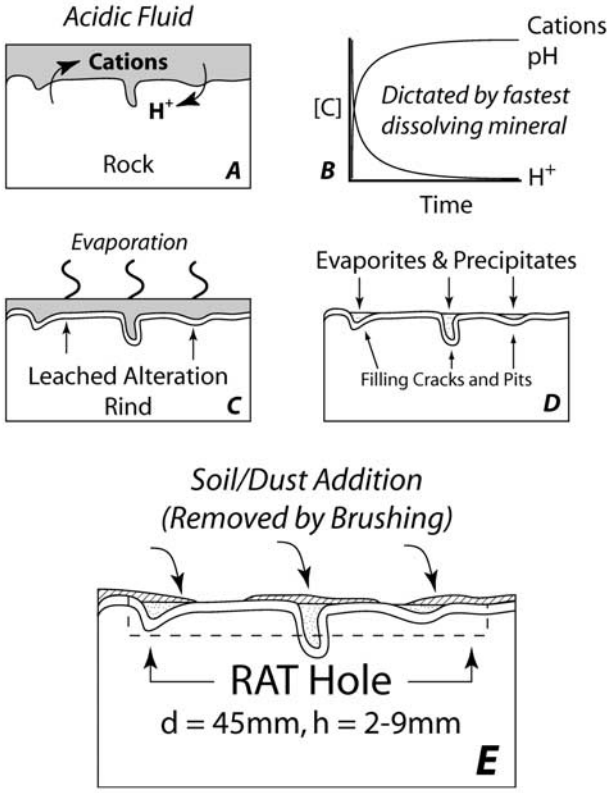

Figure 13. Schematic of alteration processes occurring at rock surfaces. (a) Rock surfaces are contacted by small volumes of acidic fluid. The fluid chemistry of the acidic fluid is dictated by interaction with the fastest dissolving mineral phase present at the rock surface, as shown in (b) a graph of concentration versus time. (c) Following reaction between acidic fluid and the rock surface, a leached alteration rind is left at the rock surface, and the fluid evaporates away. (d) Evaporite and other secondary phases are left behind and may fill cracks and pits present at the rock surface. (e) The rock is then coated by soil and/or dust, which is removed during RAT brushing operations. See text for more detailed discussion.

rock and Martian soil [*Foley et al.*, 2003; *McSween et al.*, 1999].

3.6. A Model for the Formation of Rock Surface Alteration Rinds

[39] Shown in Figures 13a–13e is a schematic illustration of a potential formation pathway for alteration rinds on rock surfaces. This model applies to the mineral dissolution and soil addition relationships discussed for the Adirondack, Clovis, Wishstone and Watchtower class rocks. In the model, small volumes of low-pH fluids contact the rock initiating mineral dissolution at the rock surface (Figure 13a). Since the observed alteration appears to be more extensive on the outer surfaces of rocks compared to rock interiors for both in-place outcrops and loose, nonoutcrop rocks, we suggest that these fluids are deposited as either (1) an acidic aerosol (so-called "acid fog") of the type proposed by *Banin et al.* [1997] and *Settle* [1979] or (2) that they may be present as thin films of water beneath snow or frost [*Arvidson et al.*, 2004], with the fluids being acidified by dissolution of previously precipitated sulfate salts present at the rock surface [*Frau*, 2000].

[40] The evolution of the chemical composition of the fluid in contact with the rock surface is shown in Figure 13b. Experimental results (discussed previously) indicate that the chemical composition of the fluid in contact with the rock surface will be dominated by whatever elements are present in the mineral phase most susceptible to acid attack. For example, if olivine dissolution dominates (as in the case of Adirondack class basalts), Mg^{2+}, Fe^{2+}, and SiO_2(aq) concentrations will increase in solution and pH levels will increase as H^+ is consumed by acid neutralization reactions between olivine and the fluid.

[41] As a result of the dissolution process, a leached alteration rind is left behind which is depleted in the elements present in the mineral phase(s) which underwent the most rapid dissolution (Figure 13c). The fluid at the rock surface then undergoes evaporation (either while still acidified, or at higher pH depending on how much H^+ has been consumed by the dissolution process), leaving behind the secondary mineral phases formed during alteration and evaporation (Figure 13d). Vugs, pits and cracks near the rock surface have been observed in MI images of the Adirondack class basalts to be filled with a bright material [*Arvidson et al.*, 2006; *Herkenhoff et al.*, 2004], possibly the secondary phases formed during alteration and evaporation. In the final step, a soil/dust coating is added to the rock surface on top of the alteration rind (Figure 13e), possibly as a result of settling onto the rock surface as airfall, or during transient burial by migrating aeolian bed forms [*Greeley et al.*, 2004].

[42] It is difficult to place meaningful constraints on the age at which the rock surfaces were altered. For the Adirondack class basalts, the age of emplacement of the cratered volcanic plains which constitute the floor of Gusev crater at Columbia Memorial Station provides an upper limit on the age of alteration. On the basis of crater counts, these basalt flows are late Hesperian to early Amazonian (~3.0 Ga) in age [*Kuzmin et al.*, 2000]. Since it appears that the alteration of these rocks is a surface effect, it is plausible that alteration occurred after these rocks had been broken into boulder form as a result of impact into a preexisting lava flow. If the alteration occurred subsequent to impact into a preexisting lava flow, alteration could have occurred at anytime subsequent to ~3.0 Ga. For rocks encountered in the Columbia Hills, the age of surface alteration could be older than ~3.0 Ga, since the emplacement of the volcanic plains postdates that of the Columbia Hills [*Arvidson et al.*, 2006].

[43] A key question with regards to the model shown in Figure 13 is: what is the source of the acidic fluid under the current dry climate regime? Supporting the idea of an "acid fog" type fluid source is the fact that Mars is known to have been volcanically active as recently as ~165Ma [*Nyquist et al.*, 2001]. It has been suggested that during periods of persistent volcanism SO_2 gas could become globally distributed on short timescales (days), be oxidized to form sulfuric acid aerosol droplets ($H_2SO_4 \cdot nH_2O$) within months to a few years, and then gravitationally settle onto the surface within a similar time period (months to a

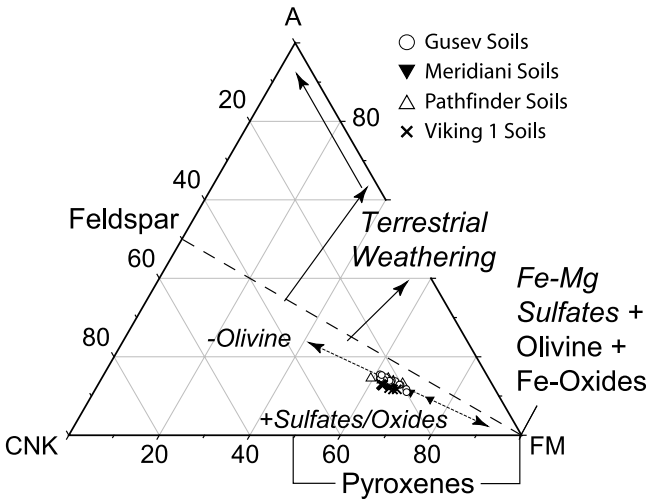

Figure 14. Ternary diagram showing soil analyses from the Spirit (white circles), Opportunity (black triangles), Pathfinder (white triangles), and Viking 1 (black crosses) landing sites. Data from *Gellert et al.* [2006], *Rieder* [2004], *Rieder et al.* [2004], *Foley et al.* [2003], and *Clark et al.* [1982].

few years) [*Settle*, 1979]. On the other hand, Mars's axial obliquity is thought to have varied on the order of 0°–60° in the past few million years [*Jakosky and Phillips*, 2001]. Modeling results suggest that at 35° obliquity (currently 25°) frost deposit thickness at Gusev crater during southern hemisphere winter would range from ~0.5–5 mm, with higher obliquity resulting in even thicker frost deposits [*Mischna et al.*, 2003], possibly supporting the idea of thin films of liquid water beneath frost deposits on rock surfaces [*Arvidson et al.*, 2004].

[44] Thus while there is no evidence to suggest that there is currently a sulfuric acid aerosol component in the Martian atmosphere, or significant frost deposition at Gusev crater, there is ample evidence to suggest that conditions have been appropriate for either, or both, of the acid sources suggested earlier to have been present in the geologically recent past. The main point is that the rock surface leaching processes discussed herein have not been extensive for any of the lithologies discussed, and rock surface–acid interactions appear to have taken place at low water to rock ratio. This indicates that whenever the surface alteration took place, it did so in a relatively dry environment, which has been the defining characteristic of Gusev Crater since at least the late Hesperian to early Amazonian [*Golombek et al.*, 2005].

3.7. Context for APXS "Surface," "Brushed," and "RATted" Analyses

[45] Our model enables one to place APXS rock analyses into a physical and geochemical context, as shown in Figure 13e. (1) The rocks analyzed by the APXS are variably coated with soil/dust, which influences the chemistry of the APXS "Surface" such that these analyses appear to be consistent with a mixture between the soil/dust coating and the underlying alteration rind. (2) The RAT brushing operation then removes the adhering soil/dust coating from the rock surface, exposing the surface immediately beneath for the APXS "Brush" analysis. In this case, the analysis is dominated by the chemistry of the leached alteration zone, produced during interaction between acidic fluids and the rock surface. The "Brush" analysis may also be variably influenced by underlying material such as unaltered rock and/or secondary minerals, and by any soil and/or dust which has not been effectively removed by the RAT brushing operation. (3) Finally, the RAT grinding operation produces a circular hole in the rock face ~45 mm in diameter, and ~5 mm deep, and the APXS is placed against the hole for an analysis of the rock interior. The APXS RATted analysis is dominated by the chemistry of the rock interior, which lies beneath the surface alteration rind. The RATted analysis may also be affected by both alteration zone chemistry (depending on the thickness of the leached zone relative to the depth of the RAT operation), any secondary minerals in the APXS field of view, and any soil/dust/RAT cuttings which have fallen into the RAT hole.

[46] The relationships shown in Figures 12a and 12b further suggest that the "Brushed" analyses may not be perfectly representative of a leached surface, and that the "RATted" analyses may not be perfectly representative of the rock interior. If the chemistry of RATted rock interiors and brushed rock surfaces differed only by the dissolution of mineral phases at the rock surface, then they would be expected to plot along the CaO+MgO to Al_2O_3 join in Figures 12a and 12b, since dissolution of olivine, pyroxene and Ca-phosphate only removes the soluble elements MgO and CaO without adding SO_3. This effect is demonstrated by the large arrowheads along the base of both figures. Instead, all of the analyses including RATted rock interiors have variable amounts of SO_3, indicating that there are either sulfate minerals present from the rock surface to the base of the RAT hole (e.g., in veins, which are visible in some MI images), and/or that soil contamination has affected all of the analyses from the rock surface to the base of the RAT-hole to variable degrees.

3.8. Martian Soil Chemistry

[47] Plotted in Figure 14 are the soil analyses from the Spirit, Opportunity, Pathfinder and Viking 1 landing sites. As indicated, the soil analyses from all of the sites align along a trend consistent with the experimental olivine-bearing basalt dissolution trend shown in Figure 4, and the Adirondack class basalt alteration trend shown in Figure 7. On the basis of this alignment one could interpret that the Martian soils represent a basaltic regolith which has undergone alteration at low pH and low water to rock ratio resulting in chemical fractionation dominated by olivine dissolution. In such a situation, more highly altered regolith samples would plot further along the olivine dissolution trend than less altered regolith samples.

[48] The process of alteration under the sulfuric acid dominated, low water to rock ratio, and evaporative conditions implicated for Adirondack class rock surfaces results primarily in the release of Mg^{2+}, Fe^{2+} and SiO_2 (aq) to solution via the rapid dissolution of olivine. Ultimately, release of these elements to solution can result in the formation of Mg sulfates, Fe sulfates and/or Fe oxides, and amorphous silica. In Figure 14, the formation of Fe and Mg sulfates, as well as Fe oxides, will result in a trend opposite to that of olivine dissolution. Therefore samples

more enriched in sulfates and/or Fe oxides will plot closer to the FeO_T + MgO apex than less enriched samples.

[49] These opposing relationships make it difficult on the basis of Figure 14 alone to determine what an individual soil analysis truly represents. Each analysis could be sampling an altered basaltic regolith which either resides with the secondary minerals formed during its alteration, or has been separated from its alteration products by physical processes (similar, by analogy, to a brushed rock surface). Alternatively, an individual soil analysis could be sampling an unaltered basaltic regolith which has been physically mixed with the secondary phases formed by alteration of basaltic materials from another location. What can be said with certainty about the relationships shown in Figure 14 is that the alignment of the soil data is consistent with olivine-bearing basalt alteration as an important control on the general geochemical characteristics of Martian soils. This alignment requires that soils be affected principally by mobility of FeO and MgO, which can be easily generated by alteration of olivine-bearing basalt at low pH and subsequent precipitation of FeO and MgO bearing secondary minerals.

[50] Taken together, the soils from four widely separated landing sites at the Martian surface do not indicate elemental fractionation patterns consistent with alteration under conditions similar to those on Earth. This can be seen by comparison to the terrestrial alteration trends shown in Figure 14. This implies that the alteration processes occurring in the equatorial regions of Mars (where complete in situ chemical analyses of rocks and/or soils have been collected) are largely characterized by interactions between low-pH fluids and basaltic rock/regolith at low water to rock ratio. We suggest that soil chemistry at the Viking 1, Pathfinder and both MER landing sites is consistent with the alteration process occurring at the microscopic scale on the surfaces of the Adirondack class basalts. If the soil-forming process on Mars were more similar to that occurring at the moderate pH and high water to rock ratio conditions endemic to planet Earth, one would expect to see chemical fractionations significantly more like those observed for terrestrial weathering profiles.

[51] It is interesting to note that if weathering via interaction with acidic fluids is an important control on the geochemistry of soils and rocks in the Martian surface environment, then carbonate minerals are not likely to be present in these deposits. Siderite ($FeCO_3$), the least soluble of the carbonate minerals, precipitates only at pH values greater than about 5, while calcite ($CaCO_3$) and magnesite ($MgCO_3$) are even more soluble [*Catling*, 1999]. Carbonate minerals would not be expected to precipitate under the acidic soil/rock alteration regime implicated herein, and any preexisting carbonates would be expected to dissolve during interaction with such fluids [*Fairen et al.*, 2004].

4. Conclusions

[52] The effects of alteration at low pH produce fundamentally different major element relationships from those observed for alteration under typical conditions on Earth. This is because at low pH, Al and Fe^{3+} are far more soluble, and the oxidation rate of Fe^{2+} to less soluble Fe^{3+} is far lower, than in the pH range of natural waters on Earth. In effect, the elements commonly taken to be immobile in terrestrial weathering profiles (Al and Fe) are mobile in the low-pH environment. Chemical fractionations observed during experimental low-pH(= 0–1) alteration of synthetic Martian basalts reveal that solution chemistry is dominated by mineral dissolution, rather than the alkali and alkaline earth element leaching associated with alteration of feldspar and other silicate minerals that is observed for moderate pH(= 5–9) weathering on Earth. The experimental data further indicate that the contribution each mineral phase makes to the solution composition is determined by their relative dissolution rates.

[53] Application of experimental results to understanding the chemistry of the surfaces of rocks exposed on the Gusev Plains and Columbia Hills indicates that the differences in chemical composition between Brushed and RATted rock analyses can be explained by low-pH mineral phase dissolution resulting from interactions between small volumes of acidic fluid and rock surfaces. In the case of the Adirondack class basalts, olivine dissolution is indicated, the Clovis class rocks may indicate pyroxene and/or basaltic glass dissolution, and the Wishstone and Watchtower class rocks indicate Ca-phosphate dissolution. In all cases, the observed differences in chemical composition are in good agreement with the dissolution behavior one would predict on the basis of relative dissolution rates and experimental data on basalt alteration at low pH. Furthermore, using the mass lost during experimental alteration of olivine-bearing basalts as a constraint, the mineral dissolution processes evident at the surfaces of Adirondack class basalts clearly occurred at low water to rock ratio and/or short cumulative duration of alteration. By inference, the same is likely to be true of the other rock surfaces discussed in this paper.

[54] The geochemistry of pristine (unbrushed, unRATted) rock surfaces can be best described as a mixture between variable amounts of adhering soil and a leached alteration rind immediately beneath the soil veneer. APXS analyses of brushed rock surfaces are dominated by the geochemistry of a leached alteration rind produced by low water to rock ratio interactions between rock surfaces and acidic fluids. The geochemistry of RATted rock surfaces appears to be relatively unaffected by these surface leaching interactions, and so the APXS RATted analyses predominantly carry the signature of rock interiors.

[55] A significant part of the chemical variation observed in Martian soils is consistent with alteration similar to that observed for the Adirondack class basalts, which is strongly influenced by the dissolution of olivine and the formation of secondary Mg (±Fe) sulfates and Fe oxides. In general, rock alteration profiles analyzed at Gusev crater, and soils analyzed at the Spirit, Opportunity, Pathfinder and Viking 1 landing sites do not mimic the chemical fractionations produced by basalt alteration on Earth, indicating they have not been altered by interaction with large volumes of moderate pH water.

[56] **Acknowledgments.** We are grateful to the entire science and engineering teams on MER who made this investigation possible. J.A.H. and N.J.T. are also indebted to the members of the Soil and Rock Physical Properties theme group, who involved us in the fascinating data returns from soil and rock analyses at Gusev crater from day one of our participation in the MER science team. Insightful reviews were provided by Jeff Taylor and Penny King. The MER project is funded by the National

Aeronautics and Space Administration. The APXS and Mössbauer instruments were funded by the German Aerospace Center (DLR). This work was also partially supported by NASA Cosmochemistry Program grant NAG5-12916 to S.M.M.

References

Arvidson, R. E., et al. (2004), Localization and physical properties experiments conducted by Spirit at Gusev crater, *Science*, *305*, 821–824.

Arvidson, R. E., et al. (2006), Overview of the Spirit Mars Exploration Rover mission to Gusev crater: Landing site to the Methuselah outcrop in the Columbia Hills, *J. Geophys. Res.*, *111*, E02S01, doi:10.1029/2005JE002499.

Banin, A., H. I. Kan, and A. Cicelsky (1997), Acidic volatiles and the Mars soil, *J. Geophys. Res.*, *102*, 13,341–13,356.

Bethke, C. M. (2002), *The Geochemist's Workbench, Release 4.0: A User's Guide to Rxn, Act2, Tact, React, and Gtplot*, 224 pp., Univ. of Ill., Urbana.

Blum, A. E., and L. L. Stillings (1995), Feldspar dissolution kinetics, in *Chemical Weathering Rates of Silicate Minerals*, edited by A. White and S. Brantley, pp. 291–352, Mineral. Soc. of Am., Washington, D. C.

Brantley, S. L., and Y. Chen (1995), Chemical weathering rates of pyroxenes and amphiboles, in *Chemical Weathering Rates of Silicate Minerals*, edited by A. White and S. Brantley, pp. 119–172, Mineral. Soc. of Am., Washington, D. C.

Burns, R. G. (1987), Ferric sulfates on Mars, *J. Geophys. Res.*, *92*, 570–574.

Burns, R. G. (1993), Rates and mechanisms of chemical weathering of ferromagnesian silicate minerals on Mars, *Geochim. Cosmochim. Acta*, *57*, 4555–4574.

Burns, R. G., and D. S. Fisher (1993), Rates of oxidative weathering on the surface of Mars, *J. Geophys. Res.*, *98*, 3365–3372.

Catling, D. C. (1999), A chemical model for evaporites on early Mars: Possible sedimentary tracers of the early climate and implications for exploration, *J. Geophys. Res.*, *104*, 16,453–16,469.

Clark, B. C., and D. C. Van Hart (1981), The salts of Mars, *Icarus*, *45*, 370–378.

Clark, B. C., A. K. Baird, R. J. Weldon, D. M. Tsusaki, L. Schnabel, and M. P. Candelaria (1982), Chemical composition of Martian fines, *J. Geophys. Res.*, *105*, 9623–9642.

Eggleton, R. A., C. Foudoulis, and V. Varkevisser (1987), Weathering of basalt: Changes in rock chemistry and mineralogy, *Clays Clay Miner.*, *35*, 161–169.

Fairen, A. G., D. Fernandez-Remolar, J. M. Dohm, V. R. Baker, and R. Amils (2004), Inhibition of carbonate synthesis in acidic oceans on early Mars, *Nature*, *431*, 423–426.

Fedo, C., H. Nesbitt, and G. Young (1995), Unraveling the effects of potassium metasomatism in sedimentary rocks and paleosols, with implications for paleoweathering conditions and provenance, *Geology*, *23*, 921–924.

Fiore, S., and R. Laviano (1991), Brushite, hydroxylapatite, and taranakite from Apulian Caves (Southern Italy)—New mineralogical data, *Am. Min.*, *76*, 1722–1727.

Foley, C. N., T. E. Economou, and R. N. Clayton (2003), Final chemical results from the Mars Pathfinder alpha proton X-ray spectrometer, *J. Geophys. Res.*, *108*(E12), 8096, doi:10.1029/2002JE002019.

Frau, F. (2000), The formation-dissolution-precipitation cycle of melanterite at the abandoned pyrite mine of Genna Luas in Sardinia, Italy: Environmental implications, *Mineral. Mag.*, *64*, 995–1006.

Gellert, R., et al. (2004), Chemistry of rocks and soils in Gusev crater from the Alpha Particle X-ray Spectrometer, *Science*, *305*, 829–832.

Gellert, R., R. Rieder, J. Brückner, B. C. Clark, G. Dreibus, G. Lugmair, D. W. Ming, H. Wanke, A. Yen, and J. Zipfel (2006), Alpha Particle X-Ray Spectrometer (APXS): Results from Gusev crater and calibration report, *J. Geophys. Res.*, doi:10.1029/2005JE002555, in press.

Gendrin, A., et al. (2005), Sulfates in Martian layered terrains: The OMEGA/Mars Express view, *Science*, *307*, 1587–1591.

Gislason, S. R., and S. Arnorsson (1993), Dissolution of primary basaltic minerals in natural-waters-saturation state and kinetics, *Chem. Geol.*, *105*, 117–135.

Gislason, S. R., and O. Eugster (1987), Meteoric water-basalt interactions. II: A field study in N. E. Iceland, *Geochim. Cosmochim. Acta*, *51*, 2841–2855.

Gislason, S. R., S. Arnorsson, and H. Armannsson (1996), Chemical weathering of basalt in southwest Iceland: Effects of runoff, age of rocks and vegetative/glacial cover, *Am. J. Sci.*, *296*, 837–907.

Golombek, M. P., J. A. Grant, L. S. Crumpler, R. Greeley, R. E. Arvidson, and the Athena Science Team (2005), Climate change from the Mars Exploration Rover landing sites: From wet in the Noachian to dry and dessicating since the Hesperian, *Proc. Lunar Planet. Sci. Conf. 36th*, *1539*.

Gorevan, S. P., et al. (2003), Rock Abrasion Tool: Mars exploration Rover mission, *J. Geophys. Res.*, *108*(E12), 8068, doi:10.1029/2003JE002061.

Greeley, R., et al. (2004), Wind-related processes detected by the Spirit Rover at Gusev crater, Mars, *Science*, *305*, 810–813.

Guidry, M. W., and F. T. Mackenzie (2003), Experimental study of igneous and sedimentary apatite dissolution: Control of pH, distance from equilibrium, and temperature on dissolution rates, *Geochim. Cosmochim. Acta*, *67*, 2949–2963.

Haskin, L. A., et al. (2005), Water alteration of rocks and soils from the Spirit rover site, Gusev crater, Mars, *Nature*, *436*, doi:10.1038/nature03640.

Herkenhoff, K. E., et al. (2004), Textures of the soils and rocks at Gusev crater from Spirit's Microscopic Imager, *Science*, *305*, 824–826.

Hurowitz, J. A., S. M. McLennan, D. H. Lindsley, and M. A. A. Schoonen (2005), Experimental epithermal alteration of synthetic Los Angeles meteorite: Implications for the origin of Martian soils and identification of hydrothermal sites on Mars, *J. Geophys. Res.*, *110*, E07002, doi:10.1029/2004JE002391.

Jakosky, B. M., and R. J. Phillips (2001), Mars' volatile and climate history, *Nature*, *412*, 237–244.

Karrat, L., A. Perruchot, and J. J. Macaire (1998), Weathering of a Quaternary glass-rich basalt in Bakrit, Middle Atlas Mountains, Morocco: Comparison with a glass-poor basalt, *Geodin. Acta*, *11*, 205–215.

Klingelhöfer, G. (2004), MER 1 Moessbauer 1 EDR V1.0, *Planet. Data Syst. Rep. MER1-M-MB-1-EDR-OPS-V1.0*, NASA.

Klingelhöfer, G., et al. (2003), Athena MIMOS II Mössbauer spectrometer investigation, *J. Geophys. Res.*, *108*(E12), 8067, doi:10.1029/2003JE002138.

Klingelhöfer, G., et al. (2004), Jarosite and hematite at Meridiani Planum from Opportunity's Mössbauer spectrometer, *Science*, *306*, 1740–1745.

Kohn, M. L., J. Rakovan, and J. M. Hughes (Eds.) (2002), *Phosphates—Geochemical, Geobiological, and Materials Importance*, *Rev. Mineral. Geochem.*, vol. 48, 742 pp., Mineral. Soc. of Am., Washington, D. C.

Kuzmin, R. O., R. Greeley, R. Landheim, N. A. Cabrol, and J. D. Farmer (2000), Geologic map of the MTM-15182 and MTM-15187 quadrangles, Gusev Crater–Ma'adim Vallis region, Mars, *U.S. Geol. Surv. Misc. Geol. Invest. Ser., Map 2666*.

McLennan, S. M. (2001), Relationships between the trace element composition of sedimentary rocks and upper continental crust, *Geochem. Geophys. Geosyst.*, *2*, doi:10.1029/2000GC000109.

McLennan, S., S. Hemming, D. McDaniel, and G. Hanson (1993), Geochemical approaches to sedimentation, provenance and tectonics, *Geol. Soc. Am. Spec. Pap.*, *284*, 21–40.

McSween, H., and K. Keil (2000), Mixing relationships in the Martian regolith and the composition of globally homogeneous dust, *Geochim. Cosmochim. Acta*, *64*, 2155–2166.

McSween, H., and A. Treiman (1998), Martian meteorites, in *Planetary Materials*, edited by J. Papike, pp. F1–F53, Mineral. Soc. of Am., Washington, D. C.

McSween, H., et al. (1999), Chemical, multispectral, and textural constraints on the composition and origin of rocks at the Mars Pathfinder landing site, *J. Geophys. Res.*, *104*, 8679–8715.

McSween, H. Y., Jr., T. L. Grove, and M. B. Wyatt (2003), Constraints on the composition and petrogenesis of the Martian crust, *J. Geophys. Res.*, *108*(E12), 5135, doi:10.1029/2003JE002175.

McSween, H. Y., et al. (2004), Basaltic rocks analyzed by the Spirit rover in Gusev crater, *Science*, *305*, 842–845.

Meyer, C. (2004), *Mars Meteorite Compendium, Astromaterials Research & Exploration Science (ARES)*, Lyndon B. Johnson Space Cent., Houston, Tex.

Michalski, J. R., M. D. Kraft, T. G. Sharp, and P. R. Christensen (2005a), Palagonite-like alteration products on the Earth and Mars I: Spectroscopy (0.4–25 microns) of weathered basalts and silicate alteration products, *Proc. Lunar Planet. Sci. Conf. 36th*, *1188*.

Michalski, J. R., M. D. Kraft, T. G. Sharp, L. B. Williams, and P. R. Christensen (2005b), Mineralogical constraints on the high-silica Martian surface component observed by TES: Clay-rich mineralogy does not sufficiently explain the Acidalia Planitia-type spectra, *Icarus*, *174*, 161–177.

Ming, D. W., et al. (2006), Geochemical and mineralogical indicators for aqueous processes in the Columbia Hills of Gusev crater, Mars, *J. Geophys. Res.*, doi:10.1029/2005JE002560, in press.

Mischna, M. A., M. I. Richardson, R. J. Wilson, and D. J. McCleese (2003), On the orbital forcing of Martian water and CO_2 cycles: A general circulation model study with simplified volatile schemes, *J. Geophys. Res.*, *108*(E6), 5062, doi:10.1029/2003JE002051.

Morris, R. V., et al. (2000), Mineralogy, composition and alteration of Mars Pathfinder rocks and soils: Evidence from multispectral, elemental and

magnetic data on terrestrial analogue, SNC meteorite, and Pathfinder samples, *J. Geophys. Res.*, *105*, 1757–1817.
Morris, R. V., et al. (2004), Mineralogy at Gusev crater from the Mössbauer spectrometer on the Spirit Rover, *Science*, *305*, 833–836.
Morris, R. V., et al. (2006), Mössbauer mineralogy of rock, soil, and dust at Gusev crater, Mars: Spirit's journey through weakly altered olivine basalt on the Plains and pervasively altered basalt in the Columbia Hills, *J. Geophys. Res.*, doi:10.1029/2005JE002584, in press.
Nesbitt, H. W., and G. Markovics (1997), Weathering of granodioritic crust, long-term storage of elements in weathering profiles, and petrogenesis of siliciclastic sediments, *Geochim. Cosmochim. Acta*, *61*, 1653–1670.
Nesbitt, H. W., and R. E. Wilson (1992), Recent chemical weathering of basalts, *Am. J. Sci.*, *292*, 740–777.
Nesbitt, H., and G. Young (1982), Early Proterozoic climates and plate motions inferred from major element chemistry of lutites, *Nature*, *299*, 715–717.
Nesbitt, H. W., and G. M. Young (1984), Prediction of some weathering trends of plutonic and volcanic rocks based on thermodynamic and kinetic considerations, *Geochim. Cosmochim. Acta*, *48*, 1523–1534.
Nesbitt, H. W., G. M. Young, S. M. McLennan, and R. R. Keays (1996), Effects of chemical weathering and sorting on the petrogenesis of siliciclastic sediments, with implications for provenance studies, *J. Geol.*, *104*, 525–542.
Newsom, H. E., J. J. Hagerty, and F. Goff (1999), Mixed hydrothermal fluids and the origin of the Martian soil, *J. Geophys. Res.*, *104*, 8717–8728.
Nyquist, L. E., D. D. Bogard, C. Shih, A. Grishake, D. Stoffler, and O. Eugster (2001), Ages and geologic histories of Martian meteorites, *Space Sci. Rev.*, *96*, 105–164.
Patchett, P., G. Ross, and J. Gleason (1999), Continental drainage in North America during the Phanerozoic from Nd isotopes, *Science*, *283*, 671–673.
Patterson, S. H. (1971), Investigations of ferruginous bauxite and other mineral resources on Kauai and a reconnaissance of ferruginous bauxite deposits on Maui, Hawaii, *U.S. Geol. Surv. Prof. Pap.*, *656*, 65 pp.
Pokrovsky, O. S., and J. Schott (2000), Kinetics and mechanism of forsterite dissolution at 25C and pH from 1 to 12, *Geochim. Cosmochim. Acta*, *64*, 3313–3325.
Rieder, R. (2004), MER 1 Alpha Particle X-Ray Spectrometer 2 EDR V1.0, *Planet. Data Syst. Rep. MER1-M-APXS-2-EDR-OPS-V1.0*, NASA.
Rieder, R., R. Gellert, J. Brückner, G. Klingelhöfer, G. Dreibus, A. Yen, and S. W. Squyres (2003), The new Athena alpha particle X-ray spectrometer for the Mars Exploration Rovers, *J. Geophys. Res.*, *108*(E12), 8066, doi:10.1029/2003JE002150.
Rieder, R., et al. (2004), Chemistry of rocks and soils at Meridiani Planum from the Alpha Particle X-ray Spectrometer, *Science*, *306*, 1746–1749.
Settle, M. (1979), Formation and deposition of volcanic sulfate aerosols on Mars, *J. Geophys. Res.*, *84*, 8343–8354.
Shellis, R. P., B. R. Heywood, and F. K. Wahab (1997), Formation of brushite, monetite and whitlockite during equilibration of human enamel with acid solutions at 37 degrees C, *Caries Res.*, *31*, 71–77.
Squyres, S. W., et al. (2004), In situ evidence for an ancient aqueous environment at Meridiani Planum, Mars, *Science*, *306*, 1709–1714.
Squyres, S. W., et al. (2006), Rocks of the Columbia Hills, *J. Geophys. Res.*, doi:10.1029/2005JE002562, in press.
Stumm, W., and J. J. Morgan (1996), *Aquatic Chemistry: Chemical Equilibria and Rates in Natural Waters*, 1022 pp., John Wiley, Hoboken, N. J.
Tang, R. K., M. Hass, W. J. Wu, S. Gulde, and G. H. Nancollas (2003), Constant composition dissolution of mixed phases II. Selective dissolution of calcium phosphates, *J. Colloid Interface Sci.*, *260*, 379–384.
Taylor, S. R., and S. M. McLennan (1985), *The Continental Crust: Its Composition and Evolution*, 312 pp., Blackwell Sci., Malden, Mass.
Tosca, N. J., S. M. McLennan, D. H. Lindsley, and M. A. A. Schoonen (2004), Acid-sulfate weathering of synthetic Martian basalt: The acid fog model revisited, *J. Geophys. Res.*, *109*, E05003, doi:10.1029/2003JE002218.
Tosca, N. J., S. M. McLennan, B. C. Clark, J. P. Grotzinger, J. A. Hurowitz, A. H. Knoll, C. Schroder, and S. W. Squyres (2005), Geochemical modeling of evaporation processes on Mars: Insight from the sedimentary record at Meridiani Planum, *Earth Planet. Sci. Lett.*, in press.
White, A. F., and S. Brantley (Eds.) (1995), *Chemical Weathering Rates of Silicate Minerals*, *Rev. Mineral.*, vol. 31, 581 pp., Mineral. Soc. of Am., Washington, D. C.
White, A. F., M. L. Peterson, and M. F. Hochella Jr. (1994), Electrochemistry and dissolution kinetics of magnetite and ilmenite, *Geochim. Cosmochim. Acta*, *58*, 1859–1875.
Wogelius, R. A., and J. V. Walther (1992), Olivine dissolution kinetics at near-surface conditions, *Chem. Geol.*, *97*, 101–112.

R. E. Arvidson, Department of Earth and Planetary Sciences, Washington University, St. Louis, MO 63130, USA.
J. A. Hurowitz, S. M. McLennan, and N. J. Tosca, Department of Geosciences, State University of New York at Stony Brook, Stony Brook, NY 11794-2100, USA. (joel.hurowitz@stonybrook.edu)
J. R. Michalski, Department of Geological Sciences, Arizona State University, Tempe, AZ 85287, USA.
D. W. Ming, NASA Johnson Space Center, Houston, TX 77058, USA.
C. Schröder, Institut für Anorganische und Analytische Chemie, Johannes Gutenberg-Universität, Staudinger Weg 9, D-55128 Mainz, Germany.
S. W. Squyres, Department of Astronomy, Cornell University, Ithaca, NY 14853, USA.